Dexterity Assessment of Fully-Actuated UAVs

Chantelle Singh, Shahab Kazemi, Joao Buzzato, and Karl Stol
Department of Mechanical and Mechatronics, University of Auckland, New Zealand.
Corresponding author Email: shahab.kazemi@auckland.ac.nz

ABSTRACT

Aerial manipulation uses unmanned aerial vehicles (UAVs) to perform interaction tasks with the environment. Many aerial applications are conducted safer and more efficient when using UAVs to replace human workers. An essential aspect of aerial manipulation is dexterity, which is generally used to describe the ability of human or robotic hands to perform tasks such as moving and rotating an object. Currently, there is limited research on the dexterity of fully-actuated UAVs. Furthermore, although there are some papers on standardized testing for aerial manipulation, there still needs to be a universally accepted method to measure dexterity or aerial manipulation capabilities in fully-actuated UAVs. This work explores the concept of dexterity in the context of fully-actuated UAVs without complex manipulator degrees of freedom (DoF) and investigates how UAV dexterity can be quantified. In this paper, three standardised UAV dexterity tests are developed and experimented on a tilted-rotor octocopter UAV to demonstrate how the feasible dexterity tests would be conducted in a controlled environment.

1 INTRODUCTION

Aerial manipulation includes a manipulator attached to a UAV hovering in the air interacting with the environment. Recently, there has been increased interest in aerial manipulation, frequently prescribed for high-altitude tasks that could be more efficient or safer than using human workers. Examples of aerial manipulation applications include canopy sampling, natural disaster clean up, high-rise window cleaning, rescue missions, and maintenance tasks [1, 2, 3].

A vital characteristic needed in manipulation is *dexterity* as described in several research studies [4, 5, 6, 7]. However, dexterity is a concept typically applied to humans and robotic hands/arms. The literature describes it as a measure of a human hand's ability to interact with the environment involving using the fingers skillfully or doing interaction tasks such as precise hand movements while manipulating objects. Despite its significance, dexterity remains a relatively unexplored characteristic in the research area of UAVs. Furthermore, more research is needed to assess the dexterity of UAVs without the added complexities introduced by multi-DoF arms.

To date, there has not yet been a standardized dexterity assessment that thoroughly examines the capabilities of fully-actuated UAVs, which have independent control of all six DoF. This study aims to quantify the dexterity of such UAVs without additional DoFs via a manipulator arm and to identify variations in dexterity across different UAVs through experimental tests. Considering the advantages and additional capabilities associated with full actuation is essential to this research. By doing so, we can compare the dexterity of different fully-actuated UAVs and identify areas where dexterity may be lacking.

Several studies have investigated human dexterity resulting in various dexterity tests available for the hand [8]. A common human dexterity test is the nine peg-in-hole test which assesses finger dexterity [9]. This test involves the human participant placing pegs in holes with a time constraint. These dexterity tests are designed to diagnose neurodegenerative diseases such as Parkinson's or multiple sclerosis, which affect a person's dexterity.

Dexterity can also be applied in the field of robotics. Researchers aim to enhance robotic hand manipulation capabilities, often comparing them to human abilities. Standardized dexterity tests have been developed that are influenced by human dexterity research to evaluate robotic arm's performance [5]. Elangovan et al. developed nineteen tests covering object manipulation and tool interaction to find an overall dexterity score. Metrics like reachable workspace and force closure are standard in dexterity research, defining the space a manipulator can access and its ability to withstand forces and torques [6, 4, 10].

An example of a standardised UAV test is seen in the study by Suarez et al. [11]. Several aspects of a UAV and manipulator arm combination were tested, such as accuracy and manipulation capability. One test involved checking that the UAV could apply force on a wall for 5 s which is similar to the force closure concept discussed previously. However, this research has several limitations, such as not focusing on dexterity and being limited to under-actuated UAV analysis.

Despite the limited availability of dexterity tests designed explicitly for UAVs and even fewer tests that do not depend on a manipulator arm, various research studies have conducted experimental tests to validate the design and control architectures of these UAVs. These tests could serve as suitable dexterity measures because they evaluate the UAV's ability to perform precise, controlled, and coordinated movements that

are helpful for manipulation. A typical experiment frequently seen in several studies is position holding, which assesses the UAV's ability to accurately maintain a specific position, reflecting its maneuverability and control precision. For example, a study by Jiang et al. [12] developed a fully-actuated hexrotor with optimized fixed tilt-rotor angles designed for aerial manipulation. The UAV experimental tests in this study show similarities to the workspace analysis in dexterity research. The test involved hovering on one spot at a roll angle with zero translation, which measures how far the UAV can reach. Kamel et al. [13] developed experimental tests involving the hexacopter rotating around one axis, which showed how the UAV was stable at different orientations. This maneuver is impossible for a typical under-actuated UAV.

Several experiments analyzed precision, which is vital for manipulation. Orsag et al. [7] examined an under-actuated quadcopter conducting insertion task using a manipulator arm. A success rate was measured in performing these tasks. However, a limitation of this research is that this test does not directly assess the dexterity of a UAV.

The concept of force closure is not usually considered for UAVs; however, it can be considered when aerial manipulation is involved. With sufficient force applied by the UAV, manipulation would be more precise because it could maintain contact and complete actions, resulting in improved dexterous manipulation. A study also conducted by Jiang et al. [14] analysed force closure and developed their UAV to instantaneously handle any wrench (combination of force and torque). In order to analyse forces and torques in each axis of the hexrotor UAV, a force/torque ellipsoid was created for rotor angles of 0º, 10º, 20º and 30º.

This paper is organised as follows. Section 2 explores what dexterity means in the context of UAVs and the requirements of a standardised UAV dexterity test. Section 3 describes the physical setup for the case study experiments conducted on a fully-actuated octocopter. This section also describes the relationships between the systems and components in this research study. Section 4 introduces the design of the dexterity tests and the experimental approach for each test. The paper then discusses the results from the case study experiments for each test in Section 5.

2 Defining Terms and Establishing a Criteria for Effective Testing

2.1 UAV Dexterity Definition

A definition of UAV dexterity can be synthesized by drawing from existing definitions for human dexterity, robotic hands, and dexterous biological aerial animals, such as hummingbirds. Hummingbirds display exceptional flight dexterity through precise hovering stability, accurate control of pitch, roll, and yaw, and the ability to dynamically adjust their body orientation. They can independently maneuver each wing, enabling sharp turns and agile navigation. This fine control is crucial for making precise contact with flowers

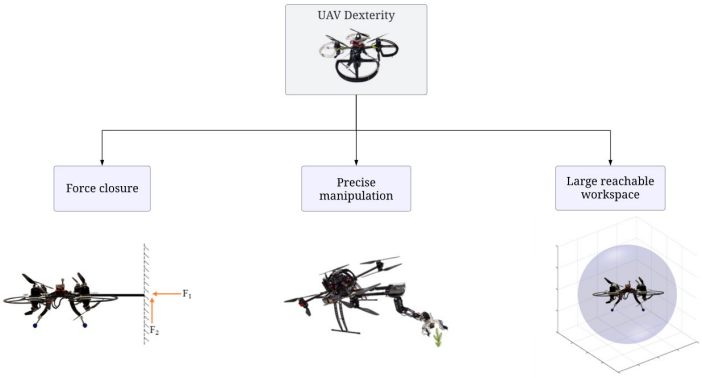

Figure 1: Conceptual framework of UAV dexterity

using their beaks, demonstrating advanced aerial manipulation. As discussed in Section 1, dexterity is a contributing factor in object manipulation skills. For UAVs designed for aerial manipulation, dexterity directly impacts proficiency in precisely handling objects during interactions.

A fundamental aspect of dexterity is force closure [10], which in the context of UAVs denotes the ability to resist external forces and torques during manipulation tasks, ensuring stable and sustained contact without slippage or loss of control over the manipulated object. Furthermore, reachability is a common consideration in robotic arm dexterity tests, as described in Section 1. The reachability of a UAV, independent of fixed manipulator arms, is helpful for its dexterity. The reachable locations are the UAV's workspace while hovering. That is, the maximum roll, pitch and yaw.

Several metrics similar to dexterity exist in the literature, such as manoeuvrability and agility [15, 16]. While these metrics contribute to UAV performance, they do not inherently encapsulate the precision and accuracy intrinsic to dexterity. Moreover, drawing inspiration from biological models, such as hummingbirds, provides valuable insights into defining UAV dexterity. Hummingbirds are known as one of the most skilful aerial manipulators in nature, as described by Haque et al. [17]. Figure 1 summarizes the definition of UAV dexterity developed in this research. This definition is utilized to create tests for measuring UAV dexterity.

2.2 Dexterity Test Requirements

To ensure compliance with existing standardized testing protocols and adequately address the unique characteristics of fully-actuated UAVs, criteria for a standardized dexterity assessment must be established. These criteria are used to develop each test, and many feasible requirements will be incorporated into the tests. According to several existing standardised testing schemes [5, 11], common characteristics involve repeatability, generalizability, affordability, and accessibility. Additionally, the dexterity tests should include being quantifiable, having a transferable score to application capability,

and being safe. Finally, the measure should be valid and reliable. Furthermore, since this research is focused on UAV dexterity, the tests also require to be independent of external attachments such as manipulator arms and therefore must not use an attachment with more that one DoF. Another aspect of this research is the test distinguishes dexterity across fully-actuated UAVs.

3 PHYSICAL SETUP AND UAV DESCRIPTION

3.1 Experimental Methods and Tools

Each experiment in this research uses several experimental tools, which are discussed in this Section. Figure 2a depicts an overview of the experimental setup. An offboard interface using MATLAB allows sending translational or rotational setpoints to the UAV. The Vicon tracker software is used as the motion capture system enabling precise tracking of the UAV's movements in 3D space. Additionally, the Vicon tracker enables relative displacements between different objects to be tracked.

The UAV chosen as a test subject is a fully-actuated octocopter (refer to Figure 4) with a co-axial stacked configuration featuring four rotors mounted on both the top and bottom levels. Each rotor is fixed at a 31 º angle, enabling a generalized wrench through the motor map. This UAV model was previously developed in a research study by Mendes Souza et. al. [18].

3.2 Relationships Between Systems

The interconnection among various systems within the experimental setup is depicted in Figure 2b. The offboard control system transmits setpoints via MAVlink User Datagram Protocol (UDP) packets, which the UAV receives through the Wi-Fi module. Subsequently, the PX4 flight controller utilizes these setpoints to command the UAV's movements during the dexterity test. Simultaneously, information regarding the UAV's spatial location, acquired through the reflective markers tracked by the motion capture cameras positioned around the laboratory, is sent back to the offboard control PC. This feedback loop enables the calculation of the distance required to reach the setpoint, allowing for adjustments to the UAV's movements until the setpoint is reached. Following each test, the flight log is downloaded for data analysis. Moreover, experimental setup in the motion capture laboratory is illustrated in Figure 2a. A PC, connected to a webcam positioned within the experimental area, also monitors the ongoing experiment. The experiment area is an enclosed netted space where the UAV tests occur.

4 DEXTERITY TESTS DESIGN

Each subsection below begins with an exploration of the rationale behind conducting the test and its significance within the context of UAV dexterity assessment. Following this, a detailed discussion of each test's design takes place. Then, a quantitative scoring metric formulation, which facilitates the standardized evaluation of UAV dexterity, is established. Furthermore, each subsection concludes with an experimental case study conducted on the fully-actuated octocopter.

4.1 Test I: Reachability

4.1.1 Test Design

The test design process draws inspiration from existing workspace analysis research of robotic arms to devise a modified test. The test looks at determining the reachable workspace of a UAV during hovering while also considering the test requirements outlined in Section 2.2. UAVs can move freely in 3D space, resulting in an effectively infinite workspace for translation. Thus, to create a test applicable to UAVs in general, the test is adapted to analyse the space reachable via rolling and pitching. The test is devised by evaluating the maximum roll and pitch angles the UAV could attain before reaching 20% away from the saturation limits. Since all UAVs can have maximum yaw (360º), yaw limits are not analysed.

This test is designed to comprehensively assess the reachable workspace of any fully-actuated UAV. It is adaptable for use on various UAV configurations, including octocopters, hexacopters or dodecacopters, which possess independent control over all six DoFs. Examining a UAV's reachable limits obtains a reachable workspace area. These limits involve determining the maximum roll and pitch angles for each combination of roll and pitch. Only a quarter of these points are determined through experiments as the UAV is symmetrical about each axis. Therefore, the negative limits are a mirror image of the positive limits.

Several data points are recorded at each limit to ensure a robust measure of the UAV's reachability workspace. These data points formed a cloud, from which a line of best fit is derived. Subsequently, an area of the first quarter of the UAV's reachability workspace is analysed to determine the score.

The scoring system is based on the area derived from the enclosure of the border of plotted roll and pitch limits calculated into a percentage as shown in Equation 1. This is to normalise the score and make it easier to compare with other UAVs.

$$R = \frac{A}{360^2} \cdot 100\% \tag{1}$$

where R is the reachability test score and A is the reachable workspace area.

The maximum score achievable is: $\frac{360^2}{360^2} \cdot 100\% = 100\%$. The score results from the fact that the maximum roll and pitch angles possible is ±180º. Therefore, the side lengths of the area graph could only range from +180 to -180 in the roll and pitch axes.

4.1.2 Experiments

Considering time constraints during experiments and the assumption that the UAV is balanced (with the CoM in the cen-

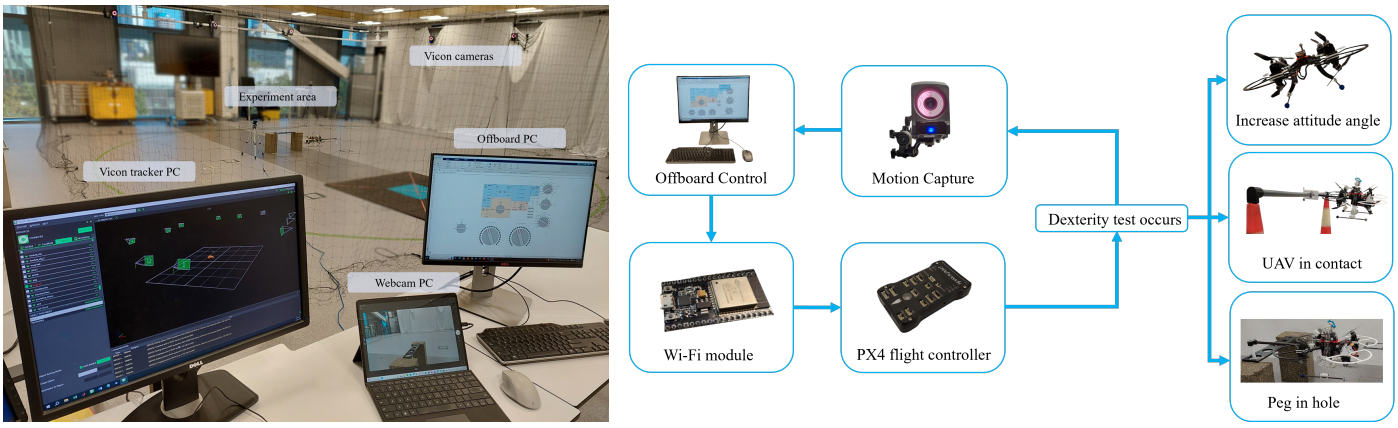

(a) Physical setup

(b) Connection between different elements used in experiments

Figure 2: Experimental setup

tre of the UAV), the roll and pitch angle limits are expected to be symmetrical at about zero. Hence, only the positive roll and pitch limits are tested, and a quarter of the reachable plot is found through experiments. Multiple tests are conducted to identify each outer limit.

The experimental procedure for this test involves using an increasing ramp signal of pitch for a constant roll angle, up to the maximum roll angle with zero pitch. The maximum pitch angle the UAV can achieve with the particular constant roll angle is reached when it utilises 80% of its thrust capability, indicating it is within 20% of its motor PWM limits.

The pitch signal rate is slow enough to allow time for the PWM signal to update on the offboard PC to be monitored by a human, ensuring that saturation is unlikely to occur. The process of monitoring PWM signals during offboard control is depicted in Figure 3 where the pitch angle at PWM levels 20% away from saturation is used as the limit. An experiment testing a high roll angle is illustrated in Figure 4a, while a test where the UAV maintains a simultaneous non-zero roll and pitch angle is depicted in Figure 4b.

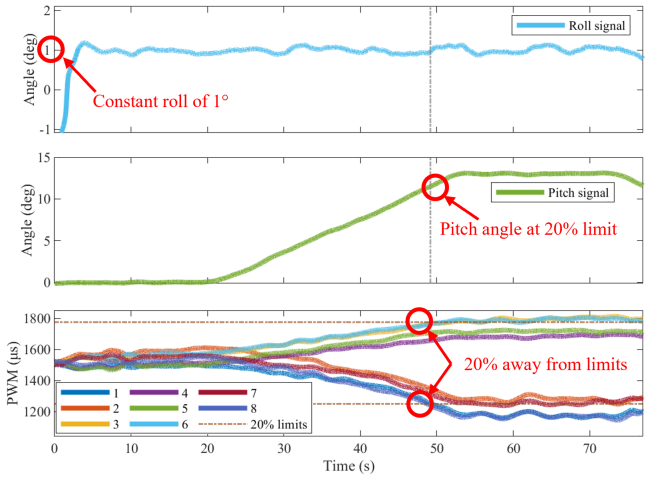

Figure 3: Finding the pitch limit for 1° roll

4.2 *Test II: Contact Testing*

4.2.1 Test Design

Several aerial manipulation applications like welding, powerline testing, and inspection using pushing mechanisms are examples of where force closure is important to consider [19, 20, 21]. This is due to the necessity of sustained contact while applying a force. The proposed test inspired by the concept of force closure discussed in Section 1, is to use a rigidly attached carbon fiber rod with an end-effector comprising a spring. The set-up and tools described in Section 3 allow for the translation of the UAV towards a flexible rod, establishing contact, and continuing to compress the spring until the

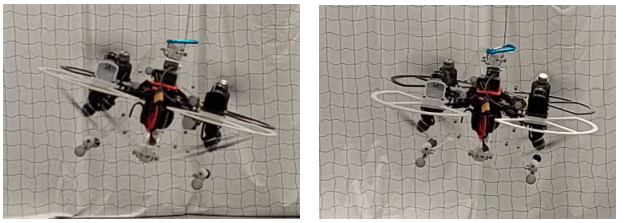

(a) High roll angle

(b) Roll and pitch angle combination

Figure 4: Experiments

PWM signals are within 30 % of their limits. The 30 % from the limits is implemented as a safety factor to avoid the UAV flipping over the contact rod if it gets too close to saturating. This choice balances demonstrating sustained force with minimizing the risk of damage posed by physical objects in the UAV experiment area. Additionally, the UAV must compress for 30 s to demonstrate stability and not instantaneously capable of applying this force. Several research studies into UAV contact testing opted to maintain contact for 10 s [21, 22]. Hence, this research chose the required contact testing time to be 30 s, emphasizing sustained contact. The spring will compress, and using motion capture technology, the displacement is measured. The compression force can be calculated with the displacement and the known spring stiffness. This experiment is repeated for 0 °, 45 °, 90 °, -45 °, and -90 ° angles. These angles are selected based on previous research on contact-based inspection UAVs [20].

The scoring system measures the force closure ability of UAVs by analysing their capacity to maintain sustained contact at different angles. The specific angles are based on their relevance to contact testing related applications, as in previous studies [20]. This test evaluates the UAV's ability to apply a force that maintains PWM signals within 30 % saturation for a sustained period, thereby quantifying the force the UAV can exert over time. Two conditions are applied to the test to analyse these characteristics. The first condition is that the compression period should exceed or equal to 30 s. Additionally, the maximum deviation in attitude angle must be below 10 °. The scoring equation is described by Equation 2.

$$C = \frac{\sum_1^5 F_n.P_n}{W} \tag{2}$$

where C is the contact test score, F_n is the force exerted by UAV at contact angle *n,* W is the UAV weight, P_n is 0 or 1 depending on whether contact testing dexterity test conditions have been met, and n is equal to 1, 2, 3, 4, or 5 (which are associated with angles 0º, 45º, 90º, -45º, -90º).

4.2.2 Experiments

The experimental setup involved the use of an acrylic interaction frame comprised five 3D-printed blocks positioned at various angles, serving to support a carbon fiber rod. Additionally, a 3D-printed end-effector was attached to the rod's end, featuring a linear spring and a sliding mechanism designed to compress the spring upon contact. The displacement of the spring could be tracked using a Vicon tracker, providing data on the compression force applied by the UAV.

The experimental procedure begins with the UAV is manually armed using a transmitter and switched to offboard control mode, where the UAV autonomously reaches the predefined set points corresponding to the rod, as determined through motion capture markers. To demonstrate sustained force within the UAV's saturation limits, a force is applied by the UAV sufficient to bring the PWM signals within 30 % saturation for a sustained period, approximately ranging between 2 and 3 N for the case study octocopter. Finally, flight log and motion capture recording data were collected to calculate the displacement of the spring on the end-effector and the coaxial compression force. Figure 5 illustrates the -45º experiment.

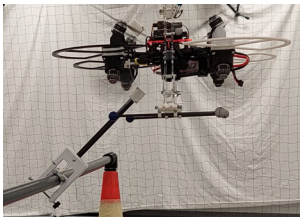

Figure 5: Experiment for -45º contact angle

4.3 Test III: Peg-in-Hole

4.3.1 Test Design

The peg-in-hole test assesses the precision of UAV operations, inspired by human peg-in-hole tasks and hummingbird dexterity in flight. The setup involves inserting a rod into an acrylic C-ring, with a 90 ° clamp angle to mimic human tests, as shown in Figure 6. A baseless hole is used to eliminate interaction effects.

Reflective motion capture markers are placed on the pegboard, and Vicon Tracker data is processed via Simulink, as depicted in Figure 2a. Consistency is maintained by using the same peg across trials, with dimensions selected based on Orsag et al. [7]. The peg, 10 % of the UAV rotor diameter (1.5 cm), is chosen to generalize across different UAVs.

Five hole sizes, ranging from 2.5 to 6.5 cm, are used to ensure test generalizability, with peg clearances from 1 to 5 cm. The pegboard is designed with CAD and 3D printed, as shown in Figure 7. The proposed approach involves waypoints using the pegboard's location coordinates, which enable the octocopter to follow a trajectory autonomously. This allows the test to be more accessible and affordable.

The test assesses the UAV system's real-time dexterity, including mechanical design, control architecture, and sensor integration, similar to human and robotic arm assessments [5]. A weighted scoring metric emphasizes precision, with higher weights for smaller holes. The peg-in-hole score is the cumulative success rate for each hole, weighted by hole size.

Specific conditions refine the test for fully-actuated UAVs, ensuring horizontal thrust is required without pitching or rolling. One condition involves translating a distance at least D_Y over 5 s or less, scaled to twice the propeller diameter (Figure 6). A second condition sets an RMSE threshold of 5 ° for horizontal thrust motion. These parameters focus on fully-actuated UAV qualities, making the test sensitive to dexterity variations across UAVs. The peg-in-hole score is detailed in Equation 3.

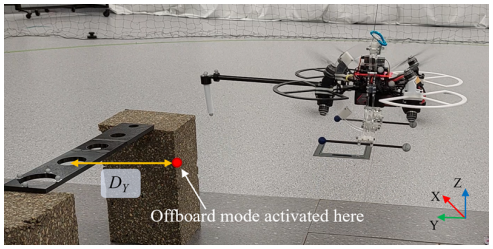

Figure 6: Illustration of conditions

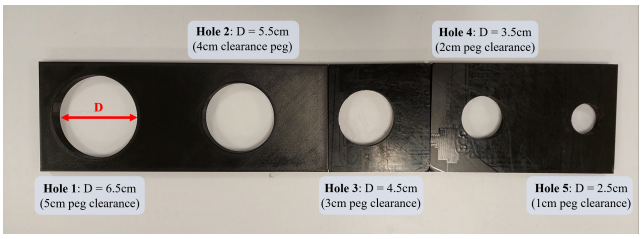

Figure 7: UAV pegboard designed for a 1.5 cm diameter peg

$$P = \sum_{1}^{5} w_u.S_u \tag{3}$$

where P is the peg-in-hole score, w_u is the weighting for peg-in-hole test, S_u is the success rate for peg-in-hole test, and u is 1, 2, 3, 4, or 5 corresponding to the pegboard hole.

From this equation it can be seen that the maximum score possible is $1 \times 100\,\% + 2 \times 100\,\% + 3 \times 100\,\% + 4 \times 100\,\% + 5 \times 100\,\% = 15$.

4.3.2 Experiments

The experiment commences by having a pegboard between two foam blocks before placing four markers around hole 1. The difference in X-axis (horizontal) displacement between each hole is added to the setpoint for the other pegboard holes. Subsequently, an object representing the UAV and the pegboard itself is created in the Vicon tracker. Assumptions regarding tuning are that the UAV being tested is tuned for free flight.

Furthermore, a marker is placed on the bottom of the peg to enable the peg's position using the Vicon tracker system to be located. This information is used in the Simulink interface to integrate the difference in the Y-axis pegboard location and peg location into offboard setpoints.

Upon completion of the setpoint configuration, the UAV is manually armed and transitioned into offboard mode, initiating autonomous navigation towards the designated hole. Following this, a stabilization period of at least two seconds is allowed before providing a Z-axis setpoint.

The setup is monitored throughout the experiment via a webcam, as depicted in Figure 2a. If the UAV deviates from its intended setpoints and makes contact with the pegboard, corrective measures are conducted to reposition the UAV.

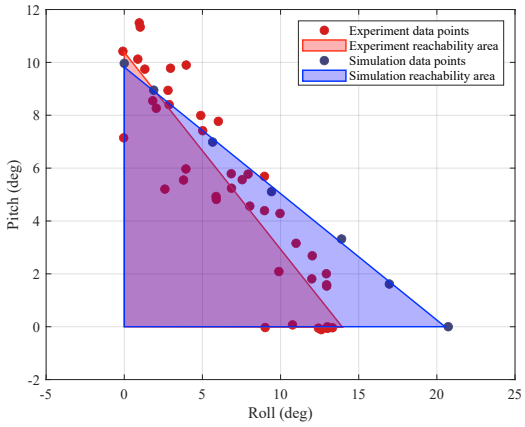

Figure 8: UAV Experiment vs Simulation Reachability Plot

5 RESULTS AND DISCUSSION

5.1 *Octocopter UAV Reachability*

Multiple experiments are conducted for each roll angle and a pitch limit found to form a cloud of points. A line of best fit is plotted in MATLAB to create the reachable workspace area. The octocopter in this study achieved an area of 71^{o^2} for the quarter reachability workspace illustrated in Figure 8 and consequently a dexterity score of: $\frac{4 \times 71.28}{360^2} \times 100\,\% = 0.22\,\%$. Comparatively, the simulation for this UAV using a quarter of the data achieving an area of 100^{o^2}, and a dexterity score of: $\frac{4 \times 100.44}{360^2} \times 100\,\% = 0.31\,\%$.

The results from this reachability test experiment provide an interpretation of the UAV's workspace that it can reach independently of a complex DoF arm. The experimental results closely resemble a simulated reachability dataset for the case study octocopter. As expected, the simulation's rolling capability is much higher, given that various factors in the experiment could reduce the UAV's thrust capability, such as motor heating and battery age. Interestingly, the experimental data for the simulation in the pitch limits is higher. This discrepancy is unexpected and could be attributed to the uncertainty in experimental data due to uncontrollable factors.

5.2 *Octocopter UAV Contact Test*

The case study octocopter is capable of successful contact for each angle assessed. The force data obtained calculates the average force exerted over the 30 s compression period. Moreover, the UAV maintained an attitude where the RMSE for all tests remained below 10 °.

Utilizing the collected data and Equation 2, a contact testing score of 1.01 is calculated for the octocopter weighing 1275 g. These results demonstrate the UAV's capability to sustain a force ranging from 2 to 3 N, while utilizing up to 80

% or more of its thrust capacity for an extended duration.

The experiments and subsequent findings present a method for assessing UAV dexterity, highlighting the fully-actuated UAV's ability to withstand forces and maintain stable hovering during aerial manipulation tasks.

Understanding this score can advance UAV development for tasks such as window cleaning, where sustained force application is essential. For example, the window cleaning aerial vehicle in [23] requires different force closure requirements than that of a transmission line inspection UAV such as in [24]. This is because the typical window cleaning action requires a larger force normal to the window surface, as opposed to a transmission line application requiring a smaller force, at potentially different angles.

5.3 Octocopter UAV Peg-in-hole

The peg-in-hole test illustrated in Figure 6 consisted of five attempts for each peg angle, resulting in five success rates. The octocopter achieved success rates of 40 % for holes 1 and 2, a 20 % success rate for hole 3, and 0 % success rates for holes 4 and 5. Using Equation 3 the peg-in-hole score is calculated as: $1{\times}40\%{+}2{\times}40\%{+}3{\times}20\%{+}4{\times}0\%{+}5{\times}0\% = 1.8$. This score corresponds to 12 % of the maximum possible score of 15 (refer to Section 4.3.1).

The Y (forward) displacement from the pegboard at the point of offboard transition exceeds the required 0.3 meters for this case study, given that the octocopter's rotor diameter is 0.15 m. Therefore, the offboard PC sends a setpoint to the UAV to move a distance towards the pegboard of at least 0.3 m. Moreover, the time to cover this displacement is less than 5 s while maintaining roll, pitch, and yaw angles at approximately 0 °. These results and the attitude for the other successful attempts had low RMSE errors, indicating that the UAV is exhibiting control over six DoF since it can translate without changing attitude. If an under-actuated UAV undergoes the same tests, the attitude RMSE is likely to be significant, and therefore this would not be considered a successful attempt.

As expected, the success rate reduces with reduced hole sizes. The score of 1.8 is 12 % of the maximum score achievable, suggesting that the test can discriminate preciseness among different UAVs, however, this can only be verified once more than one UAV is assessed.

6 CONCLUSION

This study involved designing a standardised dexterity assessment for fully-actuated UAVs and evaluating the assessment's feasibility through experiments. Previously, it was difficult to identify how well a UAV would behave during aerial manipulation. This study introduced a novel perspective to the conventional analysis of UAVs, exploring a concept infrequently used within UAV research.

A definition of dexterity was created, and three comprehensive tests were designed. Furthermore, a score was created for each test, allowing the quantification and comparison across UAVs. Following the design of the tests, an in-depth experimental investigation was conducted that demonstrated how these tests would proceed with a fully-actuated octocopter UAV.

This research holds significance within the UAV community by presenting a benchmarking method for quantifying dexterity, thereby improving the assessment of aerial manipulation capabilities in UAVs. This methodology aids researchers in selecting UAVs best suited for various aerial manipulation applications, including window cleaning, sensing tasks, and powerline testing.

Future work includes implementing the tests on more UAVs, assessing the dexterity scores across UAVs, potentially developing an overall dexterity score, and demonstrating sensitivity in scores such that different UAVs could be rated on their dexterity and suitability to particular aerial manipulation applications. Furthermore, repeating these tests in different environments, such as with wind disturbances, could provide valuable insights into the dexterity of UAVs.

ACKNOWLEDGMENT

The research reported in this article was conducted as part of "Enabling unmanned aerial vehicles (UAVs) to use tools in complex dynamic environments "UOCX2104", which is funded by the New Zealand Ministry of Business, Innovation and Employment.

REFERENCES

[1] Anibal Ollero, Guillermo Heredia, Antonio Franchi, Gianluca Antonelli, Konstantin Kondak, Alberto Sanfeliu, Antidio Viguria, J Ramiro Martinez-de Dios, Francesco Pierri, Juan Cortés, et al. The aeroarms project: Aerial robots with advanced manipulation capabilities for inspection and maintenance. *IEEE Robotics & Automation Magazine*, 25(4):12–23, 2018.

[2] Yinshuai Sun, Zhongliang Jing, Peng Dong, Jianzhe Huang, Wujun Chen, and Henry Leung. A switchable unmanned aerial manipulator system for window-cleaning robot installation. *IEEE Robotics and Automation Letters*, 6(2):3483–3490, 2021.

[3] Guangying Jiang, Richard M. Voyles, and Jae Jung Choi. Precision fully-actuated uav for visual and physical inspection of structures for nuclear decommissioning and search and rescue. In *2018 IEEE International Symposium on Safety, Security, and Rescue Robotics (SSRR)*, pages 1–7, 2018.

[4] Raymond R. Ma and Aaron M. Dollar. On dexterity and dexterous manipulation. In *2011 15th International Conference on Advanced Robotics (ICAR)*, pages 1–7, 2011.

[5] Nathan Elangovan, Geng Gao, Che-Ming Chang, and Minas Liarokapis. A modular, accessible, affordable

dexterity test for evaluating the grasping and manipulation capabilities of robotic grippers and hands. In *2020 IEEE International Symposium on Safety, Security, and Rescue Robotics (SSRR)*, pages 304–310, 2020.

[6] Joe Falco, Jeremy Marvel, and Elena Messina. *A roadmap to progress measurement science in robot dexterity and manipulation*. US Department of Commerce, National Institute of Standards and Technology, 2014.

[7] Matko Orsag, Christopher Korpela, Stjepan Bogdan, and Paul Oh. Dexterous aerial robots - mobile manipulation using unmanned aerial systems. *IEEE Transactions on Robotics*, 33(6):1453–1466, 2017.

[8] Katie E. Yancosek and Dana Howell. A narrative review of dexterity assessments. *Journal of Hand Therapy*, 22(3):258–270, 2009.

[9] Peter Feys, Ilse Lamers, Gordon Francis, Ralph Benedict, Glenn Phillips, Nicholas LaRocca, Lynn D Hudson, Richard Rudick, and Multiple Sclerosis Outcome Assessments Consortium. The nine-hole peg test as a manual dexterity performance measure for multiple sclerosis. *Multiple Sclerosis Journal*, 23(5):711–720, 2017.

[10] E. Rimon and J. Burdick. On force and form closure for multiple finger grasps. In *Proceedings of IEEE International Conference on Robotics and Automation*, volume 2, pages 1795–1800 vol.2, 1996.

[11] Alejandro Suarez, Victor M. Vega, Manuel Fernandez, Guillermo Heredia, and Anibal Ollero. Benchmarks for aerial manipulation. *IEEE Robotics and Automation Letters*, 5(2):2650–2657, 2020.

[12] Guangying Jiang and Richard Voyles. Hexrotor uav platform enabling dextrous interaction with structures-flight test. In *2013 IEEE International Symposium on Safety, Security, and Rescue Robotics (SSRR)*, pages 1–6, 2013.

[13] Mina Kamel, Sebastian Verling, Omar Elkhatib, Christian Sprecher, Paula Wulkop, Zachary Taylor, Roland Siegwart, and Igor Gilitschenski. The voliro omniorientational hexacopter: An agile and maneuverable tiltable-rotor aerial vehicle. *IEEE Robotics Automation Magazine*, 25(4):34–44, 2018.

[14] Guangying Jiang and Richard M. Voyles. *Dexterous UAVs for Precision Low-Altitude Flight*, pages 207–237. Springer Netherlands, Dordrecht, 2015.

[15] Jon Verbeke and Joris De Schutter. Experimental maneuverability and agility quantification for rotary unmanned aerial vehicle. *International Journal of Micro Air Vehicles*, 10(1):3–11, 2018.

[16] Hamza Mehmood, Takuma Nakamura, and Eric N. Johnson. A maneuverability analysis of a novel hexarotor uav concept. In *2016 International Conference on Unmanned Aircraft Systems (ICUAS)*, pages 437–446, 2016.

[17] Mohammad Nasirul Haque, Bo Cheng, Bret W Tobalske, and Haoxiang Luo. Hummingbirds use wing inertial effects to improve manoeuvrability. *Journal of the Royal Society Interface*, 20(207):20230229, 2023.

[18] Pedro Henrique Mendes Souza. *Dynamics and Control of Unmanned Aerial Vehicles for Prolonged Interaction with Compliant Environments*. PhD thesis, ResearchSpace@ Auckland, 2023.

[19] Marco Tognon, Hermes A. Tello Chávez, Enrico Gasparin, Quentin Sablé, Davide Bicego, Anthony Mallet, Marc Lany, Gilles Santi, Bernard Revaz, Juan Cortés, and Antonio Franchi. A truly-redundant aerial manipulator system with application to push-and-slide inspection in industrial plants. *IEEE Robotics and Automation Letters*, 4(2):1846–1851, 2019.

[20] Robert Watson. *Unmanned Aerial Vehicles for Contact-Based Inspection*. PhD thesis, University of Strathclyde, 2023.

[21] Takahiro Ikeda, Shogo Yasui, Motoharu Fujihara, Kenichi Ohara, Satoshi Ashizawa, Akihiko Ichikawa, Akihisa Okino, Takeo Oomichi, and Toshio Fukuda. Wall contact by octo-rotor uav with one dof manipulator for bridge inspection. In *2017 IEEE/RSJ International Conference on Intelligent Robots and Systems (IROS)*, pages 5122–5127. IEEE, 2017.

[22] Karen Bodie, Maximilian Brunner, Michael Pantic, Stefan Walser, Patrick Pfändler, Ueli Angst, Roland Siegwart, and Juan Nieto. Active interaction force control for contact-based inspection with a fully actuated aerial vehicle. *IEEE Transactions on Robotics*, 37(3):709–722, 2021.

[23] Albert Albers, Simon Trautmann, Thomas Howard, Trong Anh Nguyen, Markus Frietsch, and Christian Sauter. Semi-autonomous flying robot for physical interaction with environment. In *2010 IEEE Conference on Robotics, Automation and Mechatronics*, pages 441–446, 2010.

[24] Quanwei Du, Wuzhong Dong, Wei Su, and Qi Wang. Uav inspection technology and application of transmission line. In *2022 IEEE 5th International Conference on Information Systems and Computer Aided Education (ICISCAE)*, pages 594–597. IEEE, 2022.